Characterization of Poly(norbornene) Dendronized Polymers Prepared by Ring-Opening Metathesis Polymerization of Dendron Bearing Monomers

Andreas Nyström,[†] Michael Malkoch,[†] István Furó,[‡] Daniel Nyström,[†] Kerem Unal,[§] Per Antoni,[†] George Vamvounis,[†] Craig Hawker,[⊥] Karen Wooley,[#] Eva Malmström,[†] and Anders Hult*,[†]

Department of Fibre and Polymer Technology, School of Chemical Science and Engineering, KTH, Royal Institute of Technology, SE-100 44 Stockholm, Sweden; Department of Chemistry, School of Chemical Science and Engineering, KTH, Royal Institute of Technology, SE-100 44 Stockholm, Sweden; IBM Almaden Research Center, 650 Harry Road, San Jose, California 95120; Materials Research Laboratory, University of California, Santa Barbara, California 93106; and Center for Materials Innovation and Department of Chemistry, Washington University, One Brookings Drive, Saint Louis, Missouri 63130-4899

Received May 22, 2006; Revised Manuscript Received August 15, 2006

ABSTRACT: The preparation and characterization of a series of first to fourth generation dendronized poly(norbornene)s are presented. The monomers were synthesized in a divergent fashion from 5-norbornene-2-methanol, utilizing the acetonide protected anhydride of 2,2-bis(methylol)propionic acid. The norbornenyl bearing dendrons were polymerized by ring-opening metathesis polymerization, and it was found that the Grubbs' first generation catalyst resulted in polymers with lower polydispersity compared to the materials obtained when employing the second generation catalyst. Two series of first to fourth generation polymers were characterized by DSC, SEC, and dynamic rheological measurements. In addition, it was found that the fourth generation material could form regular, porous membranes and birefringent fibers. The membranes were characterized with atomic force and optical microscopy. The birefringent fibers were analyzed with X-ray diffraction, polarized FTIR, and polarized optical microscopy.

Introduction

The interest in materials science and therapeutics derived from tunable macromolecules with addressable surfaces is ever increasing.[1−4] 2,2-Bis(methylol)propionic acid (bis-MPA) is a nontoxic and water-soluble building block that has been explored as the basis for complex macromolecules such as dendrons,[5] dendrimers,[5,6] and dendronized polymers.[7] The reasons for this are twofold: the synthetic routes to these types of macromolecules are well established and are applicable to a wide range of systems.[5−28] For example, Fréchet and co-workers recently investigated both the bioavailability and in-vivo behavior of a dendronized polymer based on a linear backbone of poly(4-hydroxystyrene) and pendant dendrons constructed from bis-MPA repeating units.[18] A positive correlation between the size of the dendronized polymer and the blood circulation time was found, making these polymers interesting candidates as drug carriers.[18] Other recently published applications for bis-MPA based complex macromolecules include multivalent dendrimers for in-vitro recognition/detection[24] and optical power limiting materials.[22]

Dendronized polymers are the newest member of the family of dendritic polymers. Formally, these polymers are a subclass of comb polymers where the linear combs have been replaced by dendrons.[29−32] Because of the steric congestion imposed by the dendrons on the backbone of these polymers, the random coil conformation may be extended to cylindrical or rodlike conformations.[29,32,33]

Dendronized polymers described in the literature have been synthesized by employing attach-to, divergent, macromonomer strategies or most recently also by various noncovalent interactions.[29,33] Of these strategies, the macromonomer methodology combined with a "living" polymerization technique offers the greatest potential of creating polymers with a high degree of structural perfection since this allows for superior control over the placement of dendrons along the backbone.[29,33] Controlled polymerization techniques such as atom transfer radical polymerization (ATRP),[34] ring-opening polymerization (ROP),[35] reversible addition−fragmentation chain transfer (RAFT) polymerization,[36] and ring-opening metathesis polymerization (ROMP)[25,37,38] have been employed for the synthesis of dendronized polymers.

ROMP of norbornenyl bearing dendrons is an attractive method for the synthesis of dendronized polymers, since the relief of ring strain in norbornenyl group results in a strong thermodynamic driving force for the polymerization.[39,40] In addition, the pendant dendrons on a poly(norbornene) dendronized polymer are placed further apart along the backbone compared to a homopolymer of vinyl functional dendrons, resulting in a less sterically demanding environment.[41] Shielding of the polymerizable group in the case of high generation monomers may inhibit polymerization, resulting in low molecular weight polymers or possibly no polymerization at all.[33] Percec et al. have thoroughly explored the concept of polymerizing self-assembling dendrons by various techniques, including ROMP, and found that the self-assembly of monomers, oligo-

[†] Department of Fibre and Polymer Technology, Royal Institute of Technology.
[‡] Department of Chemistry, Royal Institute of Technology.
[§] IBM Almaden Research Center.
[⊥] University of California, Santa Barbara.
[#] Washington University.
* Corresponding author. E-mail: andult@polymer.kth.se.

10.1021/ma061147z CCC: $33.50
Published on Web 09/14/2006

Scheme 1. Synthesis of Dendronized Macromonomers and Polymers[a]

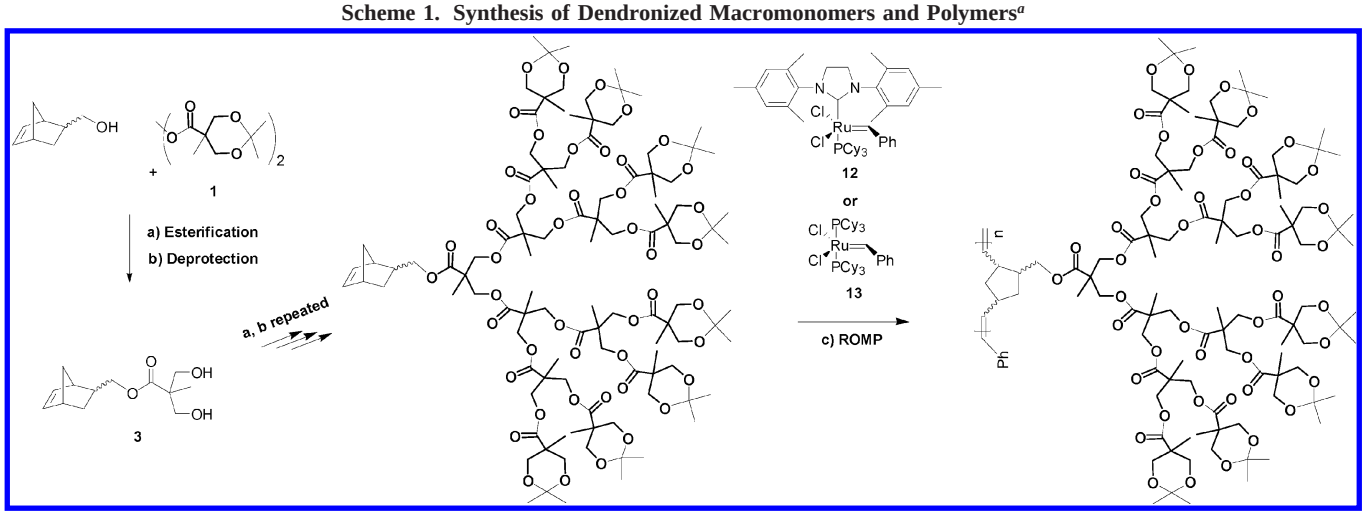

[a] Conditions: (a) DMAP, pyridine, CH_2Cl_2, RT; (b) methanol, DOWEX H^+, 40 °C; (c) 1, CH_2Cl_2 (dry), RT, 2, ethyl vinyl ether.

mers, and polymers into complex superstructures had a dramatic influence on the rate of polymerization.[37,38,42−45] However, there are only a few examples of nonassembling dendrons polymerized by ROMP in the literature.[25]

Fréchet and co-workers recently reported the preparation of diblock dendronized copolymers via ROMP of functional norbornene monomers,[25] with one block consisting of pendant fullerene units and the second block of pendant dendrons. Following this work, we wanted to explore the use of Grubbs' first and second generation catalysts for the preparation of dendronized homopolymers from bis-MPA based dendrons with norbornenyl functionality at their focal point. Furthermore, these polymers have a high functional group density at their periphery and are ideal candidates for porous membranes,[46−48] where the high functional group loading may serve as an environment for surface confined reactions and/or modifications.[49] Therefore, the porous membrane forming capabilities of these materials were investigated. The bulk properties of the dendronized polymers were also investigated in an effort to increase the understanding of the complex interplay of factors governing the properties these materials. This area of research has gained less attention compared to the effort devoted to developing new synthetic approaches to dendronized polymers[50−53] but is of importance if new applications for dendronized polymers are to be developed.

Results and Discussion

Synthesis of Macromonomers. The dendronized monomers used in this study were synthesized according to Scheme 1 starting from the commercially available 5-norbornene-2-methanol endo/exo mixture. The norbornene alcohol was chosen for two reasons: This compound has a large ring strain and can be polymerized by ROMP using Grubbs' first and second generation catalyst at room temperature.[54] Second, dendronized monomers based on this compound can be synthesized in a few steps providing a relatively simple route to these materials. The acetonide protected anhydride of bis-MPA was used as generic esterification agent for divergent dendron growth.[3,10] The acetonide protective group was removed by stirring the protected norbornenyl derivative in methanol and acidic DOWEX-50-X resin. This activated the dendron for subsequent addition of the next generation of acetonide protected bis-MPA groups.[3,10] The coupling/deprotecting reactions proved to be high yielding, and the crude monomers were purified by medium-pressure liquid chromatography eluted with a gradient of ethyl acetate and heptane.

Polymerization of Macromonomers. Grubbs' second generation catalyst has been reported to be successful for polymerizing sterically demanding norbornenyl macromonomers, despite the higher rate of propagation to rate of initiation for this catalyst system.[54−58] Since the higher generation monomers can be anticipated to be sterically demanding, this catalyst was initially tested for the polymerization. As seen in Table 1, the polymerizations with this catalyst (entries 1−8 in Table 1) resulted in polymers with rather broad polydispersities (conventional calibration 1.3−3.3, universal calibration 1.3−13) and molecular weights significantly higher than theoretical values. This indicates that there was a higher rate of propagation than initiation with this catalyst.[55−58] Therefore, the less active Grubbs' first generation catalyst was evaluated. The resulting polymers (entries 9−17 in Table 1) had comparably lower polydispersities (conventional calibration 1.1−1.3, universal calibration 1.2−3.7) and molecular weights lower than theoretical. The yields obtained for the polymers after precipitation was between 40 and 60% for all reactions. The experimentally lower molecular weight observed for these polymers are most likely related to the lower activity of the endo isomer of the norbornene toward polymerization.[54] However, the increasing size of the dendrons may also shield the polymerizable group and result in lower molecular weights as observed for other systems.[59] We were unable to calculate the theoretical molecular weight at the given conversions due to the overlapping peaks of the monomer and polymer in the ^1H NMR spectra. For all the polymers analyzed, a small high molecular weight shoulder in the SEC chromatograms was observed using the refractive index detector (conventional calibration). This shoulder was more pronounced when the viscosity detector was used (universal calibration).

As a result of the synthetic studies, the polymers prepared by using Grubbs' first generation catalyst were selected for further investigation, since these polymers had much lower polydispersity compared to the polymers obtained with the second generation catalyst.

Dendronized Polymer Characterization. Differential Scanning Calorimetry (DSC). The glass transition temperature (T_g) of the dendronized polymers was determined from the second heating DSC run and taken as the middle point of the transition (Table 2). Previously reported T_g values for dendronized poly(hydroxyl ethyl methacrylate) bearing bis-MPA dendrons are in the same range (∼20−30 °C)[52] as the materials in Table 2, indicating that bis-MPA based dendronized polymers are rather low T_g materials compared to dendronized polymers based on other types of dendrons. As seen in Table 2, the T_g of the

Table 1. Polymerization Details and SEC Results

entry	polymer	$[M]_0/[I]_0$	time [h]	M_n(theor) $\times 10^{-3}$	$M_n \times 10^{-3}$ [c]	PDI[c]	$M_n \times 10^{-3}$ [d]	PDI[d]
1	p-Nor-G#1	100[a]	20	28	200.6	2.8	84.8	5.9
2	p-Nor-G#2	49[a]	20	27	174.3	2.0	113.6	4.0
3	p-Nor-G#3	26[a]	20	28	381.2	1.9	100.1	11.1
4	p-Nor-G#4	20[a]	20	46	27.4	2.8	32.0	3.0
5	p-Nor-G#1	1426[a]	20	400	849.5	1.3	3231	1.3
6	p-Nor-G#2	724[a]	20	400	457.4	2.0	472.6	6.2
7	p-Nor-G#3	365[a]	20	400	258.4	3.3	84.9	13.0
8	p-Nor-G#4	175[a]	20	400	37.4	1.8	60.6	1.7
9	p-Nor-G#1	180[b]	20	51	66.5	1.9	43.7	2.1
10	p-Nor-G#2	180[b]	20	100	66.7	1.1	63.9	1.2
11	p-Nor-G#3	180[b]	20	198	64.6	1.1	68.7	1.3
12	p-Nor-G#4	180[b]	20	413	46.9	1.2	55.7	1.5
13	p-Nor-G#1	500[b]	20	140	154.6	1.7	68.1	2.8
14	p-Nor-G#2	500[b]	40	276	149.9	1.1	110.8	1.5
15	p-Nor-G#3	500[b]	60	549	170.0	1.4	152.6	2.8
16	p-Nor-G#4	500[b]	72	1146	129.1	1.4	125.3	3.7
17	p-Nor-G#4	500[b]	72	1146	118.9	1.5	130.8	3.5

[a] Grubbs' second generation catalyst [12]. [b] Grubbs' first generation catalyst [13]. [c] Conventional calibration. [d] Universal calibration.

Table 2. Thermal Properties

sample	DP[a]	DP[b]	T_g [°C]
p-Nor-G#1 [9]	237	156	33.2
p-Nor-G#1 [13]	551	243	30.4
p-Nor-G#2 [10]	121	116	17.9
p-Nor-G#2 [14]	271	201	25.4
p-Nor-G#3 [11]	59	63	24.1
p-Nor-G#3 [15]	155	139	25.1
p-Nor-G#4 [12]	21	24	22.3
p-Nor-G#4 [16]	56	55	23.0
p-Nor-G#4 [17]	52	57	22.7

[a] SEC M_n conventional calibration. [b] SEC M_n universal calibration.

dendronized polymers decreases slightly with increasing generation, from a value of around 30 °C for the first generation material to around 23 °C for the fourth generation material. In a previous study, the effect of growing larger and larger bis-MPA dendrons from a backbone of the same length was investigated, and a small increase in T_g with increasing generation was found.[52] Therefore, it is reasonable to assume that the decreased T_g observed for higher generations of the dendronized poly(norbornene) is related to the reduction in degree of polymerization (DP) with increasing generation of these materials.[51] As suggested for other types of dendronized polymers, a shorter chain length may reduce the fraction of less mobile polymer core, hence increasing the segmental mobility of the dendronized polymer even though the spatially demanding dendrons increases in size.[51] Because of the complex interplay of factors influencing the segmental mobility of these polymers, the effect of the DP on the T_g was difficult to address.

Dynamic Rheological Analysis. The bulk properties of the dendronized poly(norbornene)s were investigated by dynamic rheological measurements. As previously mentioned, the effect of larger pendant dendrons on the viscoelastic properties of these materials were complicated by the comparatively lower DP of the higher generation materials. Nonetheless, the effect of DP within each group (generation) of polymers can be accurately assessed, and we believe that investigating the relationship between the dendron size and viscoelastic properties is correct, if the discussion is limited to the general trends observed. The rheological measurements were conducted well above the glass transition of the corresponding materials, in a frequency range of 0.1−200 rad/s. The viscoelastic properties of these materials in a higher frequency range would be interesting to investigate; however, the thermal lability of acetonide protected dendritic structures above 130 °C limits the use of temperature−frequency superposition for these materials.[60]

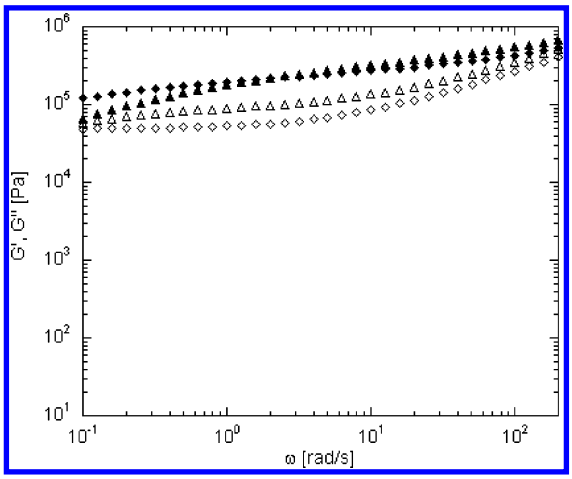

Figure 1. Storage modulus G' (filled symbols) and loss modulus G'' (open symbols) as a function of frequency (ω) for (Δ) p-Nor-G#1 [DP 237] and (◇) p-Nor-G#1 [DP 551].

The dynamic mechanical behavior in the high- and low-frequency region for the dendronized polymers reflects the glassy (high ω) and liquidlike properties (low ω) of the material, and the behavior in between these frequencies can be correlated to the structure of the polymer.[51] Figure 1 displays the frequency dependence of the storage modulus (G') and loss modulus (G'') at 80 °C for the p-Nor-G#1 polymers (entries 9 and 13 in Table 1). As seen in the figure, the dependence of the G' and G'' with increasing DP was rather weak. For the p-Nor-G#2 material (entries 10 and 14 in Table 1) in Figure 2, a stronger dependence of the DP on the G' and G'' was observed. The G' and G'' values drops significantly more with decreasing frequency for the lower DP material, and this material also displays one G'/G'' crossover in the high-frequency range. Typically, G' G'' crossover points are related to deformation rates that are in the same range as the segmental relaxation of a polymer. One can also observe that the higher DP G#2 material has one crossover in the high-frequency range and one in the low. The crossover in the high-frequency region is probably related to relaxation of the pendant dendrons, and the crossover in the lower frequencies is likely related to the backbone relaxation. A similarly strong dependence of the DP can be observed in the case of the p-Nor-G#3 samples in Figure 3 (entries 11 and 15 in Table 1), where the G' and G'' of the high DP material do not drop as much as the low DP material. One can also observe that the crossover at the lower frequencies for the high DP material was shifted toward higher frequencies compared to the p-Nor-G#2 material.

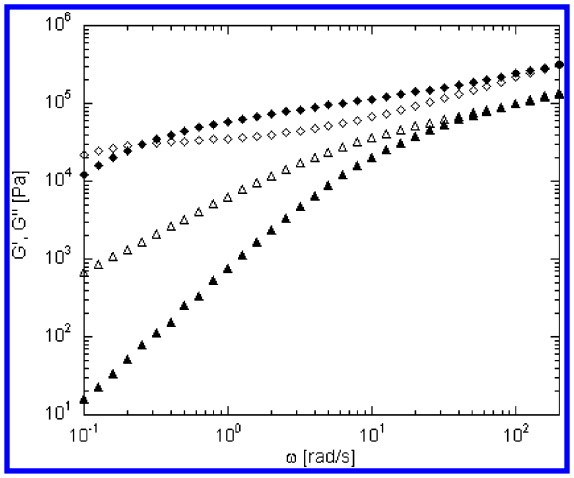

Figure 2. Storage modulus G' (filled symbols) and loss modulus G'' (open symbols) as a function of frequency (ω) for (△) p-Nor-G#2 [DP 121] and (◇) p-Nor-G#2 [DP 271].

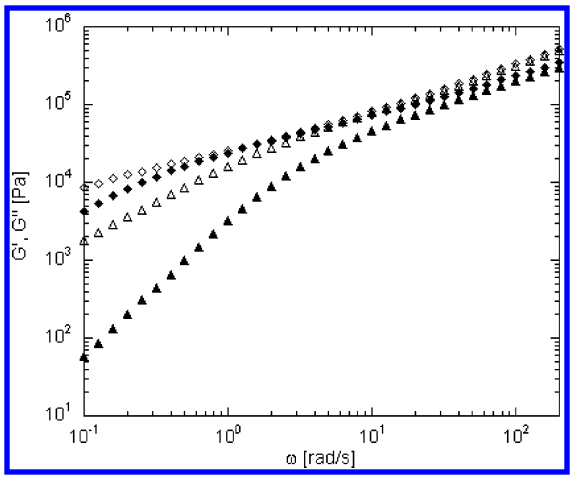

Figure 3. Storage modulus G' (filled symbols) and loss modulus G'' (open symbols) as a function of frequency (ω) for (△) p-Nor-G#3 [DP 59] and (◇) p-Nor-G#3 [DP 155].

The p-Nor-G#4 materials (entries 12 and 16 in Table 1) behave in a similar way, with a weak effect on the G' and G'' for the lower DP material, but without an observable crossover in the tested frequency range.

When comparing the G' and G'' in Figures 1−4, one observes a strong effect on the viscous (G') and elastic (G'') contribution to the complex modulus when going from the first generation material to higher generations. Previous studies on low DP dendronized polymers have suggested the size of the pendant dendrons mainly affect the G' part of the complex modulus,[53] and as seen for the lower DP materials in Figures 2−4, a comparable effect can be observed. However, in the case of the higher DP polymers, the effect of dendron size on the viscous and elastic contributions was much stronger in the lower frequency range. The slopes of the G' and G'' are similar for the higher DP p-Nor-G#2, G#3, and G#4 materials, indicating a similar relaxation behavior but with the limiting values at low frequencies differing considerably more than for the low DP polymers.

Complex Viscosity. In a previous study the complex viscosity behavior of three sets of dendronized polymers (second to fourth generation bis-MPA dendrons) having the same backbone length and different end groups was investigated. It was observed that the dendron generation had a pronounced effect on the complex viscosity as a function of frequency.[52] Increasing the dendron size from generation two to four led to a change from a

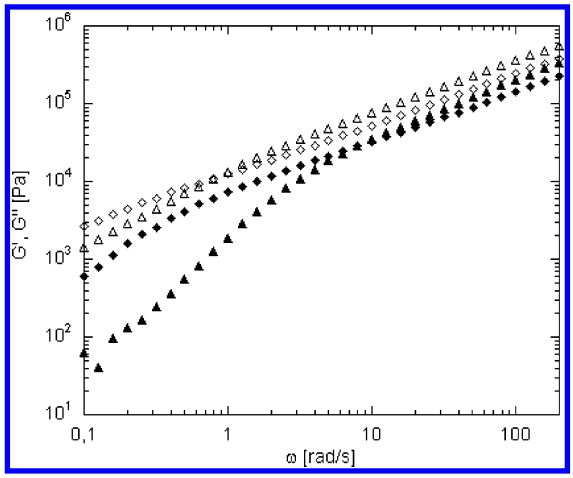

Figure 4. Storage modulus G' (filled symbols) and loss modulus G'' (open symbols) as a function of frequency (ω) for (△) p-Nor-G#4 [DP 21] and (◇) p-Nor-G#4 [DP 56].

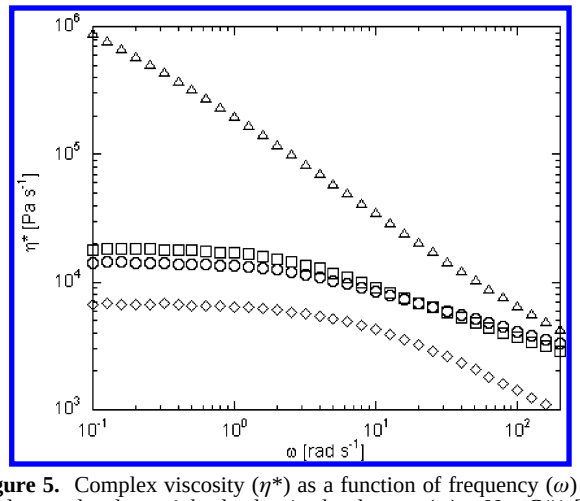

Figure 5. Complex viscosity (η^*) as a function of frequency (ω) for the low molecular weight dendronized polymers (△) p-Nor-G#1 [DP 237], (◇) p-Nor-G#2 [DP 121], (□) p-Nor-G#3 [DP 59], and (○) p-Nor-G#4 [DP 21].

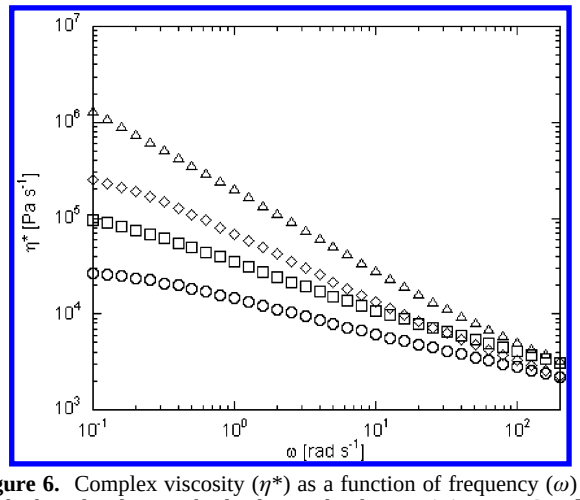

Figure 6. Complex viscosity (η^*) as a function of frequency (ω) for the high molecular weight dendronized polymers (△) p-Nor-G#1 [DP 551], (◇) p-Nor-G#2 [DP 271], (□) p-Nor-G#3 [DP 155], and (○) p-Nor-G#4 [DP 56].

Newtonian to a "shear thinning" flow behavior, with the level of the complex viscosity determined by the polarity of the end groups. Figures 5 and 6 depicts the frequency dependence of the complex viscosity at 80 °C for the two sets of first to fourth generation dendronized polymers: first set (entries 9−12 in Table 1); second set (entries 13−16 in Table 1). As seen in

Figure 5, p-Nor-G#1 is shear thinning in the whole frequency spectrum tested. When increasing the generation from one to two, there is a pronounced drop in complex viscosity in the low-frequency range and the material exhibited a Newtonian plateau, after which it becomes shear thinning. Increasing the generation to three and four increases the plateau, and the samples become shear thinning at higher frequencies. When comparing these materials with the second set of dendronized poly(norbornene)s, depicted in Figure 5, one can clearly see a different rheological behavior. The first generation samples in Figures 5 and 6 shows the same complex viscosity as a function of frequency behavior, shear thinning in the whole frequency range tested, and similar limiting complex viscosity values in the low- and high-frequency regions. The Newtonian plateaus in the low-frequency region observed for the second, third, and fourth generation materials in Figure 5 are not as pronounced in Figure 6, and the limiting values of the complex viscosity at low frequencies follows the order p-Nor-G#1 > G#2 > G#3 > G#4. We believe that the lowering of the limiting value in the low-frequency region with increasing generation of the dendronized polymers in Figure 5 is mainly an effect of the decreasing DP for the higher generation polymers. Previously published work has shown that higher generation dendronized polymers of the same backbone length has a higher limiting complex viscosity in the low-frequency region.[52] The observed differences in the rheological behavior for the second, third, and fourth generation materials in Figures 5 and 6 may be explained by the presence of chain entanglements, since the dendronized polymers in this study lack groups capable of forming secondary bonds that would result in a non-Newtonian flow behavior. Jahromi et al. suggested that the average molecular weight between two neighboring entanglements increases as the effective shielding of the backbone by the pendant dendrons increases with size.[53] Hence, the low DP p-Nor-G#2 sample depicted in Figure 5 has a DP too low to effectively entangle, whereas the higher DP p-Nor-G#2 material in Figure 6 can entangle. This conclusion is supported by the presence of a clear G'/G'' crossover in the lower frequency range for the high DP p-Nor-G#2 sample in Figure 2, indicating the formation of a physical network. The same can be seen for the p-Nor-G#3 samples. However, as seen in Figure 4, the p-Nor-G#4 samples both lack a G'/G'' crossover and their rheological behavior is quite different, but as seen in Figures 2 and 3, the G'/G'' crossover gradually increases to higher frequencies with increasing generation; a crossover for the higher DP p-Nor-G#4 sample may be present at higher frequencies than tested, but as previously mentioned, the thermal stability of dendronized polymers limits the possibility for frequency−temperature superposition to high frequencies.

^{1}H NMR Diffusion Measurements. Stimulated-echo experiments provided the diffusional decays for the investigated polymers. As described by the well-known Stejskal−Tanner formula,[61] the decays are Gaussian for polymers of narrow size distribution. This behavior was found by good approximation in sample G#2, while samples G#1 and G#4 deviated strongly from it, which is conventionally interpreted as a consequence of sizable polydispersity. To be able to perform quantitative comparisons, only the initial (down to 60% of intensity) decays were fitted[61] to provide the mass average of the diffusion coefficients that are presented in Table 3.

The observed diffusion coefficients for samples G#1 and G#2 provided, within the framework of the Kirkwood model for the diffusion of rigid-rod-like objects, unphysically small (on the order of 1 Å or below) polymer radii. This indicates that those polymers are not rodlike in THF but probably random coils with smaller corresponding hydrodynamic radius. For sample G#3, the same model provided unphysically large (>100 Å) diameters which can be explained as a sign of large polymer−polymer obstruction.[65,66] Implicitly, this finding indicates that G#3 polymers have an extended rodlike conformation since otherwise obstruction would not be significant at the explored 1% volume fraction. Since G#4 polymers are shorter, the obstruction effect that is steeply length dependent is smaller, and therefore a substantial upper limit for the hydrodynamic radius r can be calculated.

Table 3. Average Diffusion Coefficients by ^{1}H NMR and Molecular Dimensions

sample	$M_n \times 10^{-3}$ [a]	$\langle D \rangle$ [10^{-11} m^2 s^{-1}]	DP[a−c]	r [Å][c,d]
poly-Nor-G#1 [13]	154.6	11.8	551	not rodlike
poly-Nor-G#2 [14]	149.9	5.1	271	not rodlike
poly-Nor-G#3 [15]	170.0	2.3	155	
poly-Nor-G#4 [16]	129.1	5.6	56	<17

[a] THF-SEC conventional calibration. [b] Under the assumption of 2.85 Å length per unit. [c] Radius of the rodlike polymer evaluated by Kirkwood model,[62,63] assumed length obtained from SEC (for samples [13−15]) or AFM (for sample [16], see below) data. [d] The viscosity THF-d_8 is set to 0.52 cP[64] at the experimental temperature of 293 K.

AFM Imaging. AFM imaging showed well-separated single entities with a height of 1.26 ± 0.12 nm and a width of 24.8 ± 3.4 nm determined from cross-sectional analysis. It is a well-known artifact of AFM that the apparent width is measured to be larger than the real one for samples with dimensions comparable to the end radius of the AFM probe. A simple calculation[67] of the tip convolution assuming that the sample and the end radius of the AFM probe are both spheres shows that the measured width is larger than the one calculated using the measured height and the reported radius of curvature of the AFM probes used in this study (10 nm). It is then deduced that the molecules are lying on the surface with a strong interaction with the mica surface. From the measured width and by approximating the tip broadening, we estimate that the width of the molecules range from 15 to 20 nm.

Casting of Honeycomb Patterned Porous Membranes. Since François et al.[47,48,68] discovered the technique of using condensed water droplets as sacrificial templates for the formation of highly ordered porous membranes from polymers solutions, a variety of polymeric architectures have been found to form such structures.[46,69−71] For instance, Xi et al.[49,72] have shown that amphiphilic diblock copolymers composed of poly(ethylene oxide)-*block*-poly(dendronized methacrylate) can form porous membranes when cast on a variety of surfaces. In this study, nonamphiphilic dendronized homopolymers were investigated for the formation of ordered honeycomb structures. The dendronized poly(norbornene)s are interesting candidates for ordered porous membranes because of their high functional group loading at the periphery, which may serve as environment for surface confined reactions and/or modifications. Initially the first, second and third generation dendronized polymers (entries 13−15 in Table 1) were tested at different concentrations, 2−10 mg mL^{-1}, and relative humidity in the range of 50−80%, but regular structures could not be obtained. However, the fourth generation dendronized polymer (entry 17 in Table 1) readily formed ordered porous membranes when cast onto glass surfaces from $CHCl_3$ under humid conditions. Figure 8 depicts an optical microscopy image of an ordered membrane obtained when casting a 10 mg mL^{-1} solution at 22 °C and 62% RH. It can be seen that the membrane consists of hexagonally close-packed pores of uniform size. The film formation was negatively

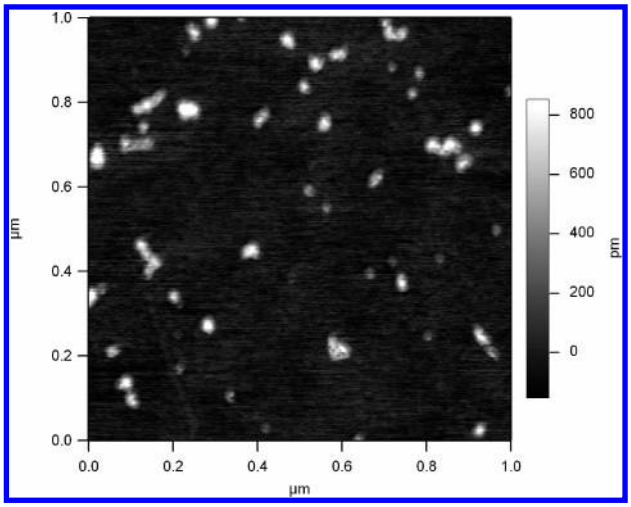

Figure 7. AFM image of p-Nor-G#4.[17]

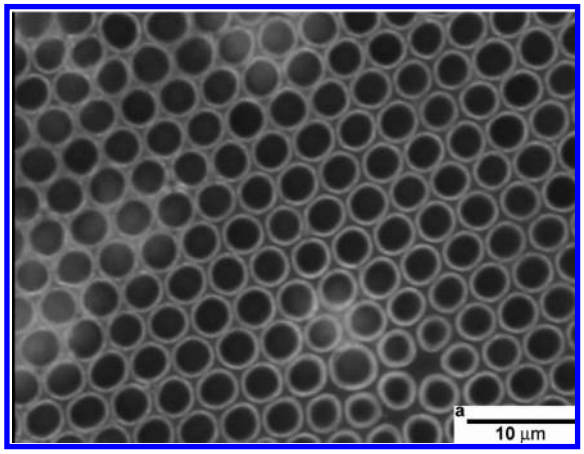

Figure 8. Example of a membrane with average pore size 3 μm, casting conditions 10 mg mL^{-1} of polymer in $CHCl_3$, 62% RH, 22 °C, ~60 μL solution applied.

effected when the concentration of the dendronized poly(norbornene) was changed from 10 mg mL^{-1} and resulted in less ordered membranes. It was also observed that the films lost their structure with time, most likely due to the low T_g of the corresponding polymer, which is close to room temperature.

The wettability of a porous and a nonporous membrane was also investigated. The nonporous membrane was obtained when a solution of the dendronized poly(norbornene) was drop cast in absence of humidity. For the nonporous surface a contact angle (CA) of ~76° against water was observed. A more hydrophobic nature was obtained for the porous membrane with a CA ~120°, and similar observations have been done by Shimomura and co-workers.[73] The enhanced CA can explained by the fact that air is trapped in between the water droplet and pore and also that the accessible surface area for a water droplet decreases at a porous surface compared to a smooth surface.

To further elucidate the topography of the porous structure, the membrane in Figure 8 was studied by AFM. The AFM was performed in noncontact mode on a 20 μm by 20 μm section of the membrane, and the resulting image and topography are depicted in Figure 9. As seen in Figure 9, the membrane has a smooth surface in between the pores; also, the three-dimensional shape of the pore (originating from the condensed water droplets) was clearly observed. The average pore size was 3 μm, which is in good agreement with the size obtained from optical microscopy, and the depth of the pore is ~1 μm (Figure 9, bottom). In addition to the polymers synthesized here, the

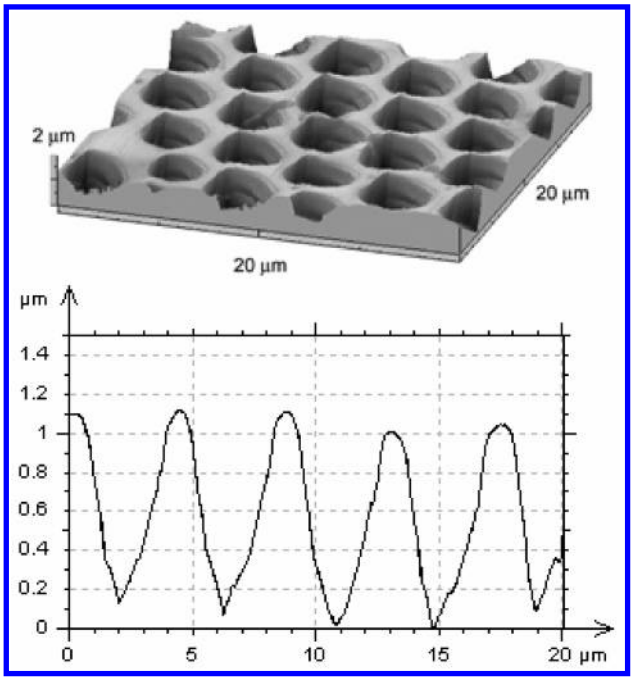

Figure 9. Top: AFM image of a 20 μm by 20 μm area of membrane (a) in Figure 8. Bottom: AFM topography image of a row of pores.

membrane forming capability of other dendronized polymers synthesized in this research group was also investigated. Similarly to the low generation dendronized polymers in this study, it was found that only the high generation dendronized poly(acrylates and methacrylates) could form porous films but these films were highly irregularly shaped.[14,21]

Birefringent Fibers from Dendronized Polymers. Fibers from dendronized polymers with pendant self-assembling dendrons that introduce order in bulk state have been reported previously.[50,74] Depending on the type of self-assembling dendrons, dendronized polymers with a range of shapes have been utilized.[37,43,45,50,74−78] However, the dendronized polymers in this study are low T_g amorphous materials without any structural moieties that can induce self-assembly. Surprisingly, long stable fibers (>40 cm) were formed from the p-Nor-G#4 (entry 17 in Table 1) material, when the parallel plate setup was retracted at 80 °C during the rheological investigations. Figure 10 shows optical microcopy images taken of a fiber using crossed polarizers and a λ-plate. The fiber was prepared by first melting ~100 mg of the fourth generation sample at 100 °C where after fibers were drawn from the melt. As seen in Figure 10, the fiber was birefringent and has a higher refractive index perpendicular to the fiber axis. Spin-cast films of the same material did not show any evidence of birefringence, and the lower generation materials could not be stretched into long thin fibers (>40 cm) without breaking.

To further investigate the observed birefringence, polarized attenuated total reflection Fourier transform infrared spectroscopy (polarized ATR-FTIR) and XRD measurements were conducted on the samples. The benefit of using polarized ATR-FTIR is that the orientation of selected bands in the polymer can be assessed.[79,80] If one assumes that the induced orientation is mainly due to backbone rearrangements, the vibrations in the fingerprint region of the IR spectra specifically related to the backbone should yield valuable information. Examples of such vibrations are the cis (~730 cm^{-1}) and trans (960 cm^{-1}) out-of-plane bending vibrations for the HC−CH double bond in the polymer backbone.[81] Figure 11 displays the polarized IR spectra of this region for the fiber (top) and the unoriented

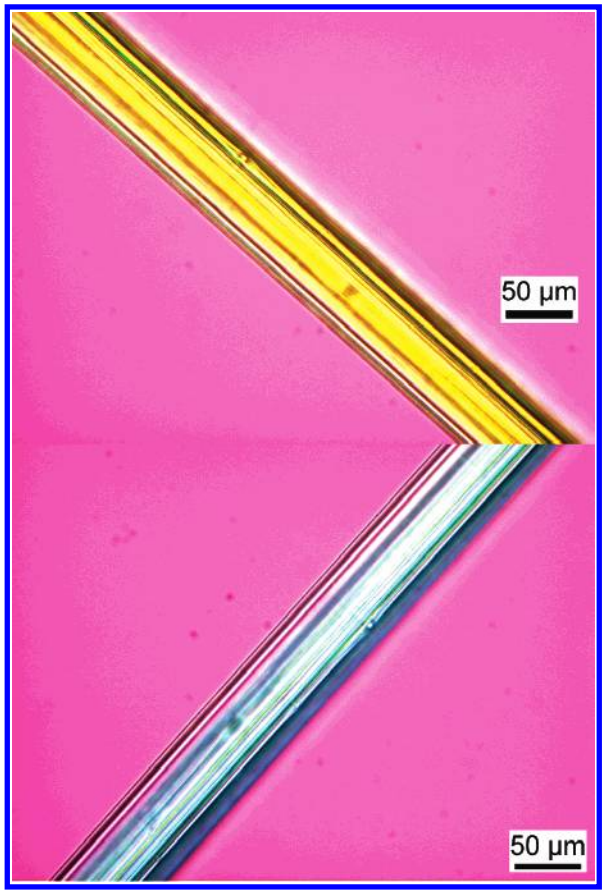

Figure 10. Polarized optical microcopy images of a fiber from p-Nor-G#4.[17] Image taken with crossed polarizers, 16× magnification, and λ-plate. (a) Fiber rotated 45° left from director. (b) Fiber rotated 315° left from director.

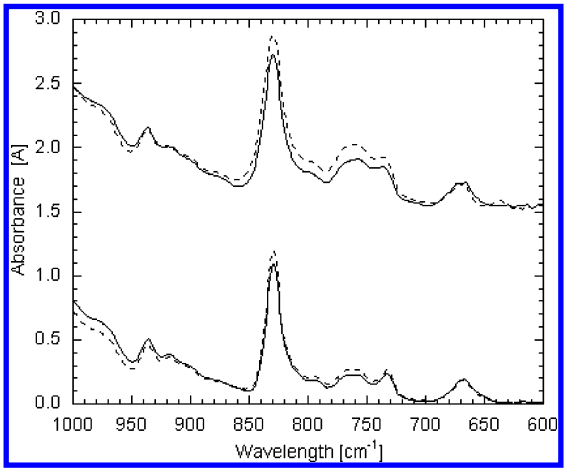

Figure 11. Polarized attenuated total reflection Fourier transform infrared (ATR-FTIR) spectra of a fiber (top) from p-Nor-G#4[17] and unoriented material (bottom). Dashed line absorption parallel to the fiber direction; solid line absorption perpendicular.

material (bottom) where the dashed line represent the absorption parallel ($A_{||}$) to the director (placed in the fiber direction) and the solid line the absorption perpendicular ($A_{\perp}$) to the fiber. The curves were normalized with respect to the absorption of the carbonyl peak, since it can be assumed that the ester groups in this highly branched polyester architecture will have no preferred orientation. The dichroic ratio (R) is defined as $R = A_{||}/A_{\perp}$ and can be used to calculate the Hermans orientation function f,[82] given that the dichroic ratio (R_0) for a perfect uniaxial orientation is known. R_0 is related to the angle α between the dipole moment vector of the vibration and the chain axis by $R_0 = 2 \cot^2 \alpha$.

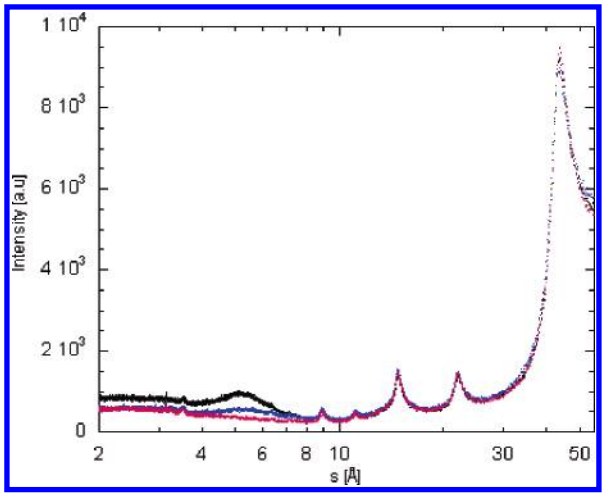

Figure 12. XRD diffractogram of a fiber from p-Nor-G#4,[17] where the red line is the fiber oriented perpendicular to the source of irradiation.

Since this angle is difficult to determine experimentally, we choose just to compare the values of the dichroic ratio for the bulk material and the fiber at the cis and trans vibrations. The cis vibration results in a dichroic ratio for the fiber, $R_{F-cis} \sim 1.24$ and $R_{B-cis} \sim 1.09$, indicating that the cis portion of the backbone was more oriented in the fiber direction. Looking at the trans vibration, one can see a weaker increase of the dichroic ratio between the unoriented material $R_{B-trans} \sim 0.86$ and the fiber $R_{F-trans} \sim 0.94$.

The fibers were also analyzed by XRD, and the diffractograms of the fiber oriented parallel and perpendicular to the source of irradiation and the unoriented material are presented in Figure 12. For both the orientation directions of fiber and the bulk material, intense peaks corresponding to distances of ∼43, ∼22, and ∼14.5 Å were found, with less intense peaks at ∼11 and 9 Å and a halo around 5 Å. As seen in Figure 12, the sharp reflections are of the same magnitude for all samples, with a more pronounced halo for the unoriented material being the only difference observed, suggesting that the amorphous content of the fiber is lower.[50]

Conclusions

Grubbs' first and second generation catalysts have been utilized for the polymerization of a set of first to fourth generation dendron bearing norbornenes. The functionalized norbornene derivatives were prepared in a divergent fashion utilizing the acetonide protected anhydride of 2,2-bis(methylol)-propionic acid. The first generation Grubbs' catalyst resulted in polymers with comparably lower polydispersity than the polymers obtained with the second generation catalyst, but with molecular weights lower than the theoretical value.

DSC analysis of the two sets of first to fourth generation dendronized poly(norbornenes) prepared with Grubbs' first generation revealed that the T_g's observed were in the range of 293−303 K for all samples, indicating that bis-MPA based dendronized polymers are low T_g materials compared to polymers with other types of dendrons.

The dynamic rheological measurements revealed that both DP and the size of the pendant dendrons affected the complex modulus. In the case of the low DP polymers, the G' part of the complex modulus was mostly affected by increasing size of the dendrons. The slopes of the G' and G'' are similar for the higher DP p-Nor-G#2, G#3, and G#4 materials, which suggest that they have a comparable relaxation behavior but

with the limiting values at low frequencies differing considerably more than for the low DP polymers.

A pronounced effect of degree of polymerization on the complex viscosity as a function of frequency was also found. The second, third, and fourth generation materials with lower DP's displayed Newtonian behavior from the lowest frequencies up to a certain limit after which they became shear tinning. The sample set of higher DP displayed shear thinning at much lower frequencies for all generations.

The porous membrane forming properties of the dendronized poly(norbornene) were investigated, and it was found that only the p-Nor-G#4 material could form regularly ordered membranes as revealed by optical and atomic force microscopy. The porous membrane also exhibited a higher water contact angle compared to regular drop-cast films due to its higher surface area.

It was found that the fourth generation dendronized polymers could be drawn to long, thin, birefringent fibers as revealed by polarized microscopy. When investigating these fibers by polarized FTIR, it was found that the backbone of the polymer was more oriented in the fiber direction. Further analysis by XRD revealed several sharp peaks for both the oriented fiber and the bulk material. The fiber material exhibited a less pronounced halo, suggesting a lower "amorphous" content in the oriented material. The nature of the birefringance and the corresponding structures to the XRD reflections are currently under further investigation.

Acknowledgment. Financial support by the Swedish Research Council under Grants 2002-5719 and 2005-6169, Wilhem Beckers Jubileumsfond, Kami Foundation, U.S. National Science Foundation Grant DMR-0301822, and The Research Council of Norway Grant 163529/S10 are acknowledged with appreciation. Prof. Ulf Gedde and Prof. Mats Johansson are greatly acknowledged for scientific discussions and help with measurements.

Supporting Information Available: Synthetic details for the preparation and characterization of the monomers and the polymers. This material is available free of charge via the Internet at http://pubs.acs.org.

References and Notes

(1) Lee, C. C.; MacKay, J. A.; Fréchet, J. M. J.; Szoka, F. C. *Nat. Biotechnol.* **2005**, *23*, 1517−1526.
(2) Gillies, E. R.; Fréchet, J. M. J. *Drug Discov. Today* **2005**, *10*, 35−43.
(3) Gillies, E. R.; Fréchet, J. M. J. *J. Am. Chem. Soc.* **2002**, *124*, 14137−14146.
(4) Hawker, C. J.; Wooley, K. L. *Science (Washington, D.C.)* **2005**, *309*, 1200−1205.
(5) Ihre, H.; Hult, A.; Fréchet, J. M. J.; Gitsov, I. *Macromolecules* **1998**, *31*, 4061−4068.
(6) Ihre, H.; Hult, A.; Söderlind, E. *J. Am. Chem. Soc.* **1996**, *118*, 6388−6395.
(7) Grayson, S. M.; Fréchet, J. M. J. *Macromolecules* **2001**, *34*, 6542−6544.
(8) Trollsås, M.; Hedrick, J. L.; Mecerreyes, D.; Dubois, P.; Jeroeme, R.; Ihre, H.; Hult, A. *Macromolecules* **1998**, *31*, 2756−2763.
(9) Ihre, H.; Padilla De Jesus, O. L.; Fréchet, J. M. *J. Am. Chem. Soc.* **2001**, *123*, 5908−5917.
(10) Malkoch, M.; Malmström, E.; Hult, A. *Macromolecules* **2002**, *35*, 8307−8314.
(11) Carlmark, A.; Malmström, E. E. *Macromolecules* **2004**, *37*, 7491−7496.
(12) Helms, B.; Mynar, J. L.; Hawker, C. J.; Fréchet, J. M. J. *J. Am. Chem. Soc.* **2004**, *126*, 15020−15021.
(13) Malkoch, M.; Claesson, H.; Löwenhielm, P.; Malmström, E.; Hult, A. *J. Polym. Sci., Part A: Polym. Chem.* **2004**, *42*, 1758−1767.
(14) Malkoch, M.; Carlmark, A.; Woldegiorgis, A.; Hult, A.; Malmström, E. E. *Macromolecules* **2004**, *37*, 322−329.
(15) Gillies, E. R.; Fréchet, J. M. J. *Bioconjugate Chem.* **2005**, *16*, 361−368.
(16) Gillies, E. R.; Dy, E.; Fréchet, J. M. J.; Szoka, F. C. *Mol. Pharm.* **2005**, *2*, 129−138.
(17) Helms, B.; Liang, C. O.; Hawker, C. J.; Fréchet, J. M. J. *Macromolecules* **2005**, *38*, 5411−5415.
(18) Lee, C. C.; Yoshida, M.; Fréchet, J. M. J.; Dy, E. E.; Szoka, F. C. *Bioconjugate Chem.* **2005**, *16*, 535−541.
(19) Malkoch, M.; Schleicher, K.; Drockenmuller, E.; Hawker, C. J.; Russell, T. P.; Wu, P.; Fokin, V. V. *Macromolecules* **2005**, *38*, 3663−3678.
(20) Mynar, J. L.; Choi, T.-L.; Yoshida, M.; Kim, V.; Hawker, C. J.; Fréchet, J. M. J. *Chem. Commun.* **2005**, 5169−5171.
(21) Nyström, A.; Hult, A. *J. Polym. Sci., Part A: Polym. Chem.* **2005**, *43*, 3852−3867.
(22) Vestberg, R.; Nilsson, C.; C.; L.; Lind, P.; B, E.; E, M. *J. Polym. Sci., Part A: Polym. Chem.* **2005**, *43*, 1177−1187.
(23) Yoshida, M.; Fresco, Z. M.; Ohnishi, S.; Fréchet, J. M. J. *Macromolecules* **2005**, *38*, 334−344.
(24) Wu, P.; Malkoch, M.; Hunt, J. N.; Vestberg, R.; Kaltgrad, E.; Finn, M. G.; Fokin, V. V.; Sharpless, K. B.; Hawker, C. J. *Chem. Commun.* **2005**, 5775−5777.
(25) Ball, Z. T.; Sivula, K.; Fréchet, J. M. J. *Macromolecules* **2006**, *39*, 70−72.
(26) Lee, C. C.; Fréchet, J. M. J. *Macromolecules* **2006**, *39*, 476−481.
(27) Vestberg, R.; Nyström, A.; Lindgren, M.; Malmström, E.; Hult, A. *Chem. Mater.* **2004**, *16*, 2794−2804.
(28) Östmark, E.; Macakova, L.; Auletta, T.; Malkoch, M.; Malmström, E.; Blomberg, E. *Langmuir* **2005**, *21*, 4512−4519.
(29) Frauenrath, H. *Prog. Polym. Sci.* **2005**, *30*, 325−384.
(30) Fréchet, J. M. J. *J. Polym. Sci., Part A: Polym. Chem.* **2003**, *41*, 3713−3725.
(31) Schlüter, A. D. *Abstr. Pap. Am. Chem. Soc.* **2001**, *221st*, PMSE-163.
(32) Frey, H. *Org. Synth. Highlights IV* **2000**, 306−313.
(33) Schlüter, A. D.; Rabe, J. P. *Angew. Chem., Int. Ed.* **2000**, *39*, 864−883.
(34) Zhang, A.; Zhang, B.; Wächtersbach, E.; Schmidt, M.; Schlüter, A. D. *Chem.—Eur. J.* **2003**, *9*, 6083−6092.
(35) Lee, C. C.; Grayson, S. M.; Fréchet, J. M. J. *J. Polym. Sci., Part A: Polym. Chem.* **2004**, *42*, 3563−3578.
(36) Zhang, A.; Wei, L.; Schlüter, A. D. *Macromol. Rapid Commun.* **2004**, *25*, 799−803.
(37) Percec, V.; Schlüter, D.; Ronda, J. C.; Johansson, G.; Ungar, G.; Zhou, J. P. *Macromolecules* **1996**, *29*, 1464−1472.
(38) Percec, V.; Holerca, M. N. *Biomacromolecules* **2000**, *1*, 6−16.
(39) Grande, D.; Six, J.-L.; Breunig, S.; Heroguez, V.; Fontanille, M.; Gnanou, Y. *Polym. Adv. Technol.* **1998**, *9*, 601−612.
(40) Delaude, L.; Jan, D.; Simal, F.; Demonceau, A.; Noels, A. F. *Macromol. Symp.* **2000**, *153*, 133−144.
(41) Cheng, C.; Khoshdel, E.; Wooley, K. L. *Macromolecules* **2005**, *38*, 9455−9465.
(42) Percec, V.; Heck, J.; Tomazos, D.; Falkenberg, F.; Blackwell, H.; Ungar, G. *J. Chem. Soc., Perkin Trans. 1* **1993**, 2799−2811.
(43) Percec, V.; Johansson, G.; Ungar, G.; Zhou, J. *J. Am. Chem. Soc.* **1996**, *118*, 9855−9866.
(44) Percec, V.; Ahn, C. H.; Barboiu, B. *J. Am. Chem. Soc.* **1997**, *119*, 12978−12979.
(45) Percec, V.; Ahn, C. H.; Ungar, G.; Yeardley, D. J. P.; Möller, M.; Sheiko, S. S. *Nature (London)* **1998**, *391*, 161−164.
(46) Stenzel-Rosenbaum, M. H.; Davis, T. P.; Fane, A. G.; Chen, V. *Angew. Chem., Int. Ed.* **2001**, *40*, 3428−3432.
(47) Pitois, O.; Francois, B. *Colloid Polym. Sci.* **1999**, *277*, 574−578.
(48) Pitois, O.; Francois, B. *Eur. Phys. J. B* **1999**, *8*, 225−231.
(49) Cheng, C. X.; Tian, Y.; Shi, Y. Q.; Tang, R. P.; Xi, F. *Langmuir* **2005**, *21*, 6576−6581.
(50) Andreopoulou, A. K.; Carbonnier, B.; Kallitsis, J. K.; Pakula, T. *Macromolecules* **2004**, *37*, 3576−3587.
(51) Zhang, A.; Okrasa, L.; Pakula, T.; Schlüter, A. D. *J. Am. Chem. Soc.* **2004**, *126*, 6658−6666.
(52) Nyström, A. M.; Furó, I.; Malmström, E.; Hult, A. *J. Polym. Sci., Part A: Polym. Chem.* **2005**, *43*, 4496−4504.
(53) Jahromi, S.; Palmen, J. H. M.; Steeman, P. A. M. *Macromolecules* **2000**, *33*, 577−581.
(54) Jha, S.; Dutta, S.; Bowden, N. B. *Macromolecules* **2004**, *37*, 4365−4374.
(55) Love, J. A.; Sanford, M. S.; Day, M. W.; Grubbs, R. H. *J. Am. Chem. Soc.* **2003**, *125*, 10103−10109.
(56) Bielawski, C. W.; Grubbs, R. H. *Macromolecules* **2001**, *34*, 8838−8840.
(57) Sanford, M. S.; Love, J. A.; Grubbs, R. H. *J. Am. Chem. Soc.* **2001**, *123*, 6543−6554.
(58) Trnka, T. M.; Grubbs, R. H. *Acc. Chem. Res.* **2001**, *34*, 18−29.
(59) Schlüter, A. D. *C. R. Chim.* **2003**, *6*, 843−851.

(60) Ropponen, J.; Tuuttila, T.; Lahtinen, M.; Nummelin, S.; Rissanen, K. *J. Polym. Sci., Part A: Polym. Chem.* **2004**, *42*, 5574−5586.
(61) Stejskal, E. O.; Tanner, J. E. *J. Chem. Phys.* **1965**, *42*, 288−292.
(62) Kirkwood, J. D.; Auer, P. L. *J. Chem. Phys.* **1951**, *19*, 281−283.
(63) Teraoka, I. *Polymer Solutions*; Wiley: New York, 2002.
(64) Holz, M.; Mao, X.-a.; Seiferling, D.; Sacco, A. *J. Chem. Phys.* **1996**, *104*, 669−679.
(65) Bu, Z.; Russo, P. S.; Tipton, D. L.; Negulescu, I. I. *Macromolecules* **1994**, *27*, 6871−6882.
(66) Cobb, P. D.; Butler, J. E. *J. Chem. Phys.* **2005**, *123*, 054908/054901−054908/054919.
(67) Zenhausern, F.; Adrian, M.; Emch, R.; Taborelli, M.; Jonbin, M.; Descouts, P. *Ultramicroscopy* **1992**, *42*−*44*, 1168−1172.
(68) Widaswski, G.; Rawieso, B.; Francois, B. *Nature (London)* **1994**, *369*, 387.
(69) Stenzel, M. H. *Aust. J. Chem.* **2002**, *55*, 239−243.
(70) Nyström, D.; Antoni, P.; Malmström, E.; Johansson, M.; Whittaker, M.; Hult, A. *Macromol. Rapid Commun.* **2005**, *26*, 524−528.
(71) Sung, L.; Bly, R. K.; Wilson, J. N.; Bakbak, S.; Park, J. O.; Srinivasarao, M.; Bunz, U. H. F. *Adv. Mater. (Weinheim, Ger.)* **2004**, *16*, 115.
(72) Cheng, C.; Tian, Y.; Shi, Y.; Tang, R.; Xi, F. *Macromol. Rapid Commun.* **2005**, *26*, 1266−1272.
(73) Yabu, H.; Takebayashi, M.; Tanaka, M.; Shimomura, M. *Langmuir* **2005**, *21*, 3235.
(74) Percec, V.; Rudick, J. G.; Peterca, M.; Wagner, M.; Obata, M.; Mitchell, C. M.; Cho, W.-D.; Balagurusamy, V. S. K.; Heiney, P. A. *J. Am. Chem. Soc.* **2005**, *127*, 15257−15264.
(75) Balagurusamy, V. S. K.; Ungar, G.; Percec, V.; Johansson, G. *J. Am. Chem. Soc.* **1997**, *119*, 1539−1555.
(76) Hudson, S. D.; Jung, H. T.; Percec, V.; Cho, W. D.; Johansson, G.; Ungar, G.; Balagurusamy, V. S. K. *Science (Washington, D.C.)* **1997**, *278*, 449−452.
(77) Percec, V.; Chu, P.; Ungar, G.; Zhou, J. *J. Am. Chem. Soc.* **1995**, *117*, 11441−11454.
(78) Percec, V.; Ahn, C. H.; Cho, W. D.; Jamieson, A. M.; Kim, J.; Leman, T.; Schmidt, M.; Gerle, M.; Möller, M.; Prokhorova, S. A.; Sheiko, S. S.; Cheng, S. Z. D.; Zhang, A.; Ungar, G.; Yeardley, D. J. P. *J. Am. Chem. Soc.* **1998**, *120*, 8619−8631.
(79) Gedde, U. W.; Andersson, H.; Hellermark, C.; Jonsson, H.; Sahlen, F.; Hult, A. *Prog. Colloid Polym. Sci.* **1993**, *92*, 129−134.
(80) Chuah, H. H. *Macromolecules* **2001**, *34*, 6985−6993.
(81) Brumaghim, J. L.; Girolami, G. S. *Organometallics* **1999**, *18*, 1923−1929.
(82) Jasse, B.; Koenig, J. L. *J. Macromol. Sci., Rev. Macromol. Chem.* **1979**, *C17*, 61−135.

MA061147Z